AQUA
Water Infrastructure, Ecosystems and Society

IWA PUBLISHING

 AQUA — Water Infrastructure, Ecosystems and Society Vol 70 No 8, 1192 doi: 10.2166/aqua.2021.041

Pilot study on the treatment of lake water with algae by ultrafiltration–ozone–biologically activated carbon

Pengcheng Xu[a], Yan Chen[a,*], Bo Gui[b], Xiaolong Guo[a] and Jian Zhang[a]

[a] Key Laboratory of Yellow River Water Environment in Gansu Province, College of Environment and Municipal Engineering, Lanzhou Jiaotong University, Lanzhou 730070, China
[b] Key Laboratory of Yangtze Aquatic Environment, Ministry of Education, College of Environmental Science and Engineering, Tongji University, Shanghai 200092, China
*Corresponding author. E-mail: xiaojingmama@163.com

ABSTRACT

For the treatment of lake water with algae, the coagulation–ultrafiltration–ozone–biologically activated carbon (CUF–O_3–BAC) integrated process was first used to treat East Taihu Lake water in China, aiming at evaluating the removal efficiencies of algae, permanganate index (COD_{Mn}), UV_{254}, NH_3-N and disinfection by-products (DBPs) precursors. In addition, the long-term performance of the membrane operation under the fluxes of 60, 70, 80 and 90 L/(m^2·h) was also investigated, and kinetic models were established. The experimental results showed that the integrated process had positive impaction of algae, COD_{Mn}, UV_{254} and NH_3-N removal, and the removal rates were 95.89 ± 1.52, 76.18 ± 4.38, 72.06 ± 4.72 and 81.31 ± 6.71%, respectively. The CUF process was prone to increase the formation potentials of DBPs. Although ozone could reduce the formation risks of chlorinated trihalomethanes (THMs) to a certain extent, it is ineffective to reduce those of brominated THMs and haloacetic acids (HAA_5). However, the CUF–O_3–BAC process was an effective technology for the removal of THMs and HAA_5 precursors in drinking water treatment. Finally, it was found that the relationship between transmembrane pressure (TMP) and time conformed to the first-order and second-order kinetic models, and the linear fitting coefficients were all above 90%.

Key words: disinfection by-products (DBPs), lake water with algal, membrane fluxes, NH_3-N, ultrafiltration–ozone–biologically activated carbon (UF–O_3–BAC)

HIGHLIGHTS

- The treatment of lake water with algae by ultrafiltration–ozone–biologically activated carbon.
- Study on the removal of disinfection by-products precursors.
- The kinetic models of transmembrane pressure and running time were established.

GRAPHICAL ABSTRACT

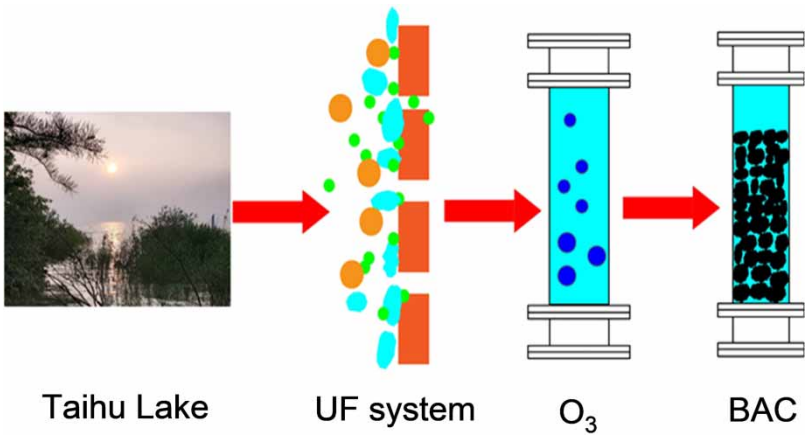

1. INTRODUCTION

Eutrophication has been affecting the water ecological health of many freshwater lakes and reservoirs in the world since the 1960s (de Oliveira *et al.* 2020). The sudden excessive growth of seasonal algae in lakes and reservoirs excessively burdens drinking water treatment plants (DWTPs) and worsens the water quality (Lin *et al.* 2018). However, conventional water treatment technologies, including coagulation, flocculation and filtration, are inefficient for removing cyanobacterial blooms and some dissolved organic matter (Bai *et al.* 2019), and even excessive algae will clog filtration tanks during the operation of waterworks (He *et al.* 2021). During the growth and death of algae, undesirable organic matter is released into the water, such as algae organic matter (AOM) (Dong *et al.* 2021). As AOM contains numerous carbohydrates, amino acids and proteinaceous compounds, all these are potential precursors of carbonaceous disinfection by-products (C-DBPs) and nitrogenous disinfection by-products (N-DBPs) (Zhu *et al.* 2015), which will cause a negative impact on subsequent treatment units and drinking water quality. According to Lui *et al.* (2011), some algal-derived organic matters with hydrophilicity and low molecular weight (MW) cannot be easily removed by flocculation/coagulation, and eventually contribute substantially to DBPs formation. Previous toxicological studies have reported that DBPs could cause public health and safety risks, so it is necessary to control them. There are a number of strategies to limit the concentrations of DBPs, such as removing the DBPs precursors before disinfection, removal of DBPs after formation or by using substitute disinfectants (Mazhar *et al.* 2020). Some studies believed that the application of reverse osmosis membranes or improved disinfection methods were effective options for controlling the formation of DBPs (Yang *et al.* 2017; Thostenson *et al.* 2018). However, costs and technologies usually limit the choice of water treatment methods. At present, an effective and economical strategy to control the formation of DBPs in DWTPs is to remove the precursors before they react with disinfectants (Chaukura *et al.* 2020).

There are quite a few strategies to solve the algae problem. Many previous studies had shown that for the treatment of water with algae, chemical pre-oxidation could change the morphology and structure of algae and reduce algal cells stability, which was very efficient for the removal of algae and also conducive to the saving of coagulants in the follow-up coagulation process (Ma & Liu 2002; Chen *et al.* 2009; Lin *et al.* 2021). Therefore, chemical pre-oxidation was once considered a promising strategy. However, excessive oxidants will also cause the release of AOM, especially intracellular organic matter (IOM) (Qi *et al.* 2016; Wang *et al.* 2021). Some references have demonstrated that IOM is an important C-DBPs and N-DBPs precursors compared with other AOM and/or natural organic matter (NOM) (Wang *et al.* 2021). In particular, the release of IOM during pre-oxidation prior to coagulation will result in the formation of more trihalomethanes (THMs) (Zhao *et al.* 2020). In terms of pre-ozonation, Dong *et al.* and Lin *et al.* reported that pre-ozonation increased the formation of haloacetic acids (HAA_5) and THMs from algae (Dong *et al.* 2021; Lin *et al.* 2021). In addition, the strong oxidizability of ozone will also destroy algal cells and make them release substances such as algal toxins and odors (e.g., 2-methylisocamphanol, 2-MIB). Although some studies have suggested that ozonation and activated carbon adsorption can effectively reduce the concentration of 2-MIB in water, this approach is not always sufficient to guarantee that the treated water concentration achieves the China potable water standard for the odor threshold (10 ng/L) (Li *et al.* 2019). Ozonation is commonly considered to be an efficient approach to remove algal toxins. However, due to the relatively complicated structure of toxins and the interference of coexisting organic compounds, it is unrealistic to thoroughly mineralize algal toxins by ozonation (Chang *et al.* 2014). Moreover, the increase of algal toxins and other substances also increased ozone consumption, which inevitably increased economic costs and resulted in the formation of DBPs (Rangesh & Sorial 2011). It is unacceptable due to economic and health concerns. Therefore, it is crucial to remove algal cells and reduce the degree of algal cell rupture in the pretreatment stage to ensure the safety of drinking water.

The coagulation–ultrafiltration process (CUF) is an efficient water treatment technology with the advantages of low cost and easy operation (Li *et al.* 2020). It can remove particles, colloids, microorganisms, pathogens and reduce transmembrane pressure (TMP) development and the extent of irreversible fouling in the UF system (Tabatabai *et al.* 2014; Li *et al.* 2020). Hence, the CUF unit is used as the pretreatment stage to remove high MW fractions and algae cells by coagulation and UF. This not only reduces the burdens of follow-up treatment but also reduces the release of IOM and other substances to the greatest extent, which plays an important role in ensuring drinking water quality. The ozone–biologically activated carbon (O_3–BAC) advanced treatment process is an advanced water purification technology because it can remove DBPs precursors, toxic pollutants and improve biostability (Wang *et al.* 2019). It has been broadly applied in DWTPs in various countries (Kim *et al.* 2005). Therefore, the coagulation–ultrafiltration–ozone–biologically activated carbon (CUF–O_3–BAC) integrated process was first used to treat East Taihu Lake water in China, aiming at evaluating the removal efficiencies of

algae, permanganate index (COD_{Mn}), UV_{254}, NH_3-N and DBPs precursors, and observing the variation of TMP under various fluxes. Finally, the ultimate purpose of this study is to provide a meaningful reference for the process improvement and research in the future from the perspectives of theory and practice.

2. MATERIALS AND METHODS

2.1. Experimental material

East Taihu Lake in China serves as the water source for the pilot device, with a scale of about 510 L/h. The raw water quality indicators are given in Table 1. The experimental parameters were previously obtained by Yin *et al.* (2019). The coagulant used in the experiment was polyaluminum chloride (PAC), and the dosage was 4 mg/L as aluminum. The membrane material was a multibore polyethersulfone hollow fiber UF membrane, using internal pressure filtration, with an effective surface area of 6.5 m^2 and a cut-off MW of 150,000 Da. The dosage of ozone was 1 mg/L, and the exposure time was 15 min. The coal-based granular activated carbon (GAC) was used as the carbon pool filter material. The depth of the carbon layer was 1 m, the filtration rate was 6.5 m/h and the empty bed exposure time was 10 min.

2.2. Analytical methods

2.2.1. General parameter analyses

As shown in Figure 1, the raw water first passed through 200 μm butterfly filter to remove large-sized suspended and floating matter, and then directly entered the UF tank after coagulation and finally entered the O_3–BAC tank. The removal efficiencies of algae, COD_{Mn}, UV_{254}, NH_3-N and DBPs precursors in the CUF–O_3–BAC integrated process were investigated. Turbidity was measured by a desktop turbidity meter (2100N, Hach, USA). The pH was measured using a pH meter (PB-21, Sartorius, Germany). COD_{Mn} was determined by the acidic potassium permanganate method. UV_{254} was measured at a wavelength of 254 nm (Evolution 200, Thermo Fisher, Germany) using a 1 cm quartz cell. The concentration of NH_3-N was determined by Nessler's reagent spectrophotometry. The instrument was a dual-beam ultraviolet-visible ultraviolet spectrophotometer (Evolution 300, Thermo Fisher, Germany).

2.2.2. DBPs analyses

All water samples were buffered with pH 7 phosphate buffer before chlorination. If necessary, the water samples were first adjusted to pH 7 with dilute sulfuric acid and/or dilute sodium hydroxide, and then buffered with pH 7 phosphate buffer. Then each sample was disinfected with sodium hypochlorite, and the dosage was 2 mg/L as Cl_2. After chlorination, the samples were incubated at constant temperature (25 ± 1 °C) for 24 h in the dark to simulate water chlorination and investigate the formation of DBPs in water samples (Prasert *et al.* 2021). The reaction was stopped after 24 h by adding excessive ascorbic acid (Watson *et al.* 2018). THMs and HAA_5 were tested using a gas chromatograph with an electron capture detector (Agilent, 7890A, USA). For THMs testing, 5 ml samples were directly taken and then placed in a gas chromatograph for determination. According to the water quality determination of HAA_5-gas chromatography (Ministry of Environmental Protection 2015), HAA_5 was extracted by the liquid/liquid technique with methyl tertiary-butyl ether followed by derivatization with acidic methanol.

Table 1 | Raw water quality indicators

Parameters	Value
Turbidity (NTU)	61.5 ± 28.35[a]
pH	7.90 ± 0.19
COD_{Mn} (mg/L)	3.67 ± 0.41
UV_{254} (cm^{-1})	0.06 ± 0.01
NH_3-N (mg/L)	0.11 ± 0.03
Phycocyanin (μg/L)	198.53 ± 66.00

[a]Mean ± standard deviation.

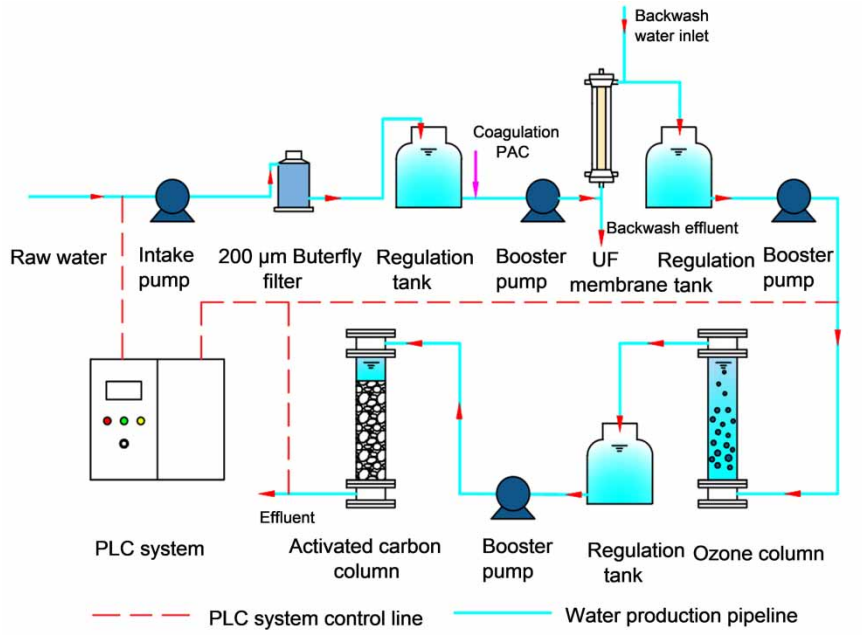

Figure 1 | CUF–O_3–BAC integrated process.

2.2.3. TMP experiments

Four different fluxes (60, 70, 80 and 90 L/(m^2·h)) were used to investigate the performance of the membrane system during long-term operation, and each operating mode was continuously operated for 30 days. Constant flux operation mode was adopted for UF. One-minute hydraulic positive flushing and one-minute hydraulic backwashing were carried out every 30 min of operation, and online chemical cleaning was used every 24 h. The changes of TMP during the experiment were automatically recorded by the PLC (Programmable Logic Controller) system.

3. RESULTS AND DISCUSSION

The average removal efficiencies of phycocyanin, COD_{Mn}, UV_{254} and NH_3-N via the CUF unit and the integrated process are shown in Figure 2.

3.1. Removal efficiency of phycocyanin

Phycocyanin is a phycobilin pigment, mainly found in cyanobacteria (Thomson-Laing *et al.* 2020). Published literature has shown that phycocyanin is an important indicator of cyanobacteria, and cyanobacterial blooms can be quickly and easily

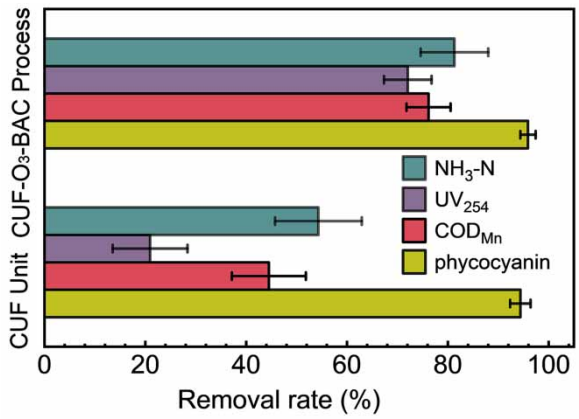

Figure 2 | Average removal efficiencies of phycocyanin, COD_{Mn}, UV_{254} and NH_3-N by the CUF unit and the integrated process.

monitored by the phycocyanin concentration (Lzydorczyk *et al.* 2009). Therefore, Phycocyanin was used to characterize the concentration of cyanobacteria in the experiment. Figure 2 shows that the removal rates of phycocyanin via the CUF unit and the integrated process reached 94.39 ± 2.03 and 95.89 ± 1.52%, respectively. It indicated that both the CUF unit and the integrated process could effectively reduce the concentration of cyanobacteria, but the CUF unit played a major role. Previous studies have shown that the algae in Taihu Lake are mainly cyanobacteria with a diameter between 2 and 15 μm, which are larger than the pore size of the UF membrane. Therefore, the UF has a good removal effect for cyanobacteria. The stimulation of ozone to algal cells was significantly reduced by this physical interception, thus reducing the release of AOM, which also indicated that the formation of DBPs could be reduced during subsequent chlorination.

3.2. Removal efficiency of COD_{Mn}

The average concentrations of COD_{Mn} in the effluent from the CUF unit and the integrated process were 2.01 ± 0.16 and 0.86 ± 0.10 mg/L, respectively, and the removal rates were 44.51 ± 7.33 and 76.18 ± 4.38%, respectively (Figure 2). It can be seen that the COD_{Mn} value of the effluent from the CUF unit has met the requirement of China's 'Standards for drinking water quality' (GB 5749-2006) of no more than 3 mg/L, indicating that the CUF unit has positive impaction of COD_{Mn} removal. The removal of COD_{Mn} via the CUF process mainly depends on the coagulation process. Because the coagulant first adsorbed the −OH group on the surface of the particulates, resulting in electric neutralization and bridging effect, and then reacted with the solution hydrolysis to produce gel precipitates, which further played the role of bonding and coagulation (Han & Huang 2013), thereby increasing the size of the organic colloid in water and making it easy to be removed via UF. Because COD_{Mn} reflects organic matter with lower MW fractions and the aperture of the UF membrane is large, the removal of COD_{Mn} via the UF membrane mainly relies on the adsorption and retention of the filter cake layers on the membrane surface and the membrane itself. The integrated process further improved the removal rate of COD_{Mn}. First, ozonation caused breakage of carbon–carbon double bonds of some organic matter, which resulted in the production of more bioavailable organic matter (Lundqvist *et al.* 2019). Therefore, the concentration of COD_{Mn} can be reduced via the role of subsequent biological activated carbon tanks.

3.3. Removal efficiency of UV_{254}

UV_{254} stands for aromatic structures of organics that are primarily humics and is sensitive to the formation of THMs (Xu *et al.* 2011, 2019), so it is necessary to control it. During the experiment, the UV_{254} value of raw water was relatively low, with an average concentration of 0.06 ± 0.01 cm^{-1}, which was mainly related to the ecological environment of the lake region. Due to the dense aquatic plants in East Taihu Lake, the hydrophilic substances after decomposition of plants, which were easily decomposed and utilized by microorganisms, were released into the aquatic environment, so the UV_{254} value of the hydrophobic substance was relatively low (Feng *et al.* 2016). As shown in Figure 2, the average removal efficiencies of UV_{254} via the CUF unit and the integrated process reached 20.94 ± 7.42 and 72.06 ± 4.72%, respectively. It indicated that the integrated process could effectively reduce the risk of DBPs formation during disinfection. Since coagulation had a good effect on the removal of macromolecules and hydrophobic organic compounds, the removal of UV_{254} via the CUF unit was mainly completed via the coagulation process. The removal rate of UV_{254} was significantly improved by the integrated process. It was because post-ozone had strong oxidizability, and it was expert in reducing humic and fulvic substances via converting them into simple non-humic forms with small molecules that were easier to biodegradation (Sun *et al.* 2018).

3.4. Removal efficiency of NH_3-N

Because East Taihu Lake is a typical grass-type lake, NH_3-N is mainly produced via the decomposition of dead aquatic plants and other residues (Fan *et al.* 2004). The experiment was carried out under the conditions of water temperature around 28 °C and pH around 8.0. Therefore, the NH_4^+ and NH_3 accounted for about 90 and 10% of NH_3-N (Zhang 2000). As shown in Figure 2, the average removal efficiencies of NH_3-N via the CUF unit and the integrated process reached 54.32 ± 8.60 and 81.31 ± 6.71%, respectively. It showed that both the CUF unit and O_3–BAC process had positive impaction of NH_3-N removal. This phenomenon seems very interesting, and the removal mechanism of NH_3-N will be discussed below. The removal mechanism of NH_3-N by the CUF unit is shown in Figure 3.

The removal efficiency of NH_3-N by coagulant was poor. This was due to the fact that metal hydroxide sols formed during coagulation carried the like charge as NH_4^+ (Wongcharee *et al.* 2020), and NH_3-N reflected small MW fractions. Therefore, the removal mechanism of NH_3-N in this experiment was mainly based on the viewpoints of Yu *et al.*, Liu *et al.* and Chen *et al.* Yu *et al.* (2020) and Liu *et al.* (2017) believed that the formation of filter cake layer on the membrane surface and the

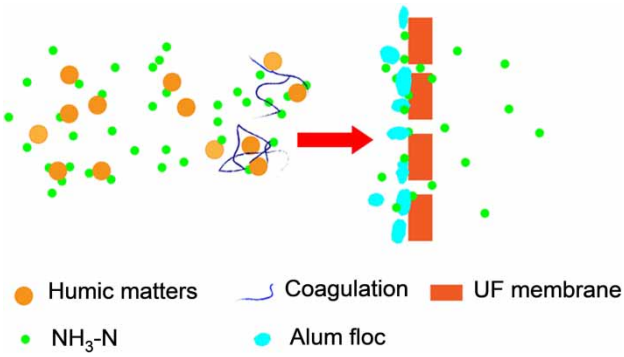

Figure 3 | Removal mechanism of NH_3-N in the CUF processs.

accumulation and growth of nitrifying bacteria could induce an effective removal of NH_4^+-N by adsorption and oxidation. Chen *et al.* (2020) considered that electrostatic attraction was the main mechanism for NH_3-N removal during the CUF, through which NH_3-N adhered to the surface of the negatively charged colloidal particles and was removed through particles discharging. In this research, these colloidal particles were more inclined to humic acid in the aquatic environment.

Some studies have shown that (Wongcharee *et al.* 2020) the NOM in water contributes to the removal of NH_3-N, among which humic acid may play a crucial role. Humic acid is a complex compound with amino acids and polysaccharides formed via lignin through a series of oxidation and demethylation processes. It contains both hydrophobic and hydrophilic parts and many chemical functional groups, such as carboxyl, phenolic, carbonyl and hydroxyl (Zhang & Bai 2003). The existence of these groups causes the acidity and exchangeability of humic acid, which can carry out ion exchange and complexation with NH_4^+ in aquatic environment, thereby promoting the adsorption of NH_4^+ (Meng *et al.* 2011). Furthermore, NH_3 can also combine with humic substances in water. Some researchers argued that a relatively small amount of quinones or phenols in humic substance would fix a large amount of NH_3, and the reaction model is shown in Figure 4 (Stevenson & Xia 1994). However, the BAC also played a positive role in the removal of NH_3-N. It is because the decomposition of ozone can provide an abundance of dissolved oxygen. Under such conditions, NH_3/NH_4^+ can be converted into NO_2^- and NO_3^- by ammonia-oxidizing microorganisms, thus further reducing the value of NH_3-N.

3.5. Effect of the integrated process on DBPs formation

To guarantee the health and safety of potable water, chlorine disinfection is commonly used to kill pathogens in potable water (Zhang *et al.* 2020). However, the existence of toxic and harmful DBPs such as THMs and HAAs in water during chlorination have aroused great concern to human health (Farré *et al.* 2011). Epidemiological studies have shown that drinking chlorinated water is associated with bladder cancer, colon cancer and rectal cancer (Pan *et al.* 2014; Chen *et al.* 2021). Therefore, it is critical to evaluate the process for the removal of DBPs. The concentrations of DBPs in influent and effluent are given in Table 2.

Figure 5 shows the removal efficiencies of THMs and HAA_5 precursors by the integrated process. Figure 5(a) shows that the CUF process could only reduce the formation potential of TCM, but only about 0.76%. The occurrence of this phenomenon may be related to the characteristics of organic matter in water. It is because UF usually exhibited better removal efficiency for high MW fractions, which is relatively poor for low and medium MW fractions. Some studies have reported that the small and medium MW fractions are major DBPs precursors (Yan *et al.* 2010; Xu *et al.* 2019). Generally, the higher MW fractions of NOM are more aliphatic, while the lower MW fractions contain more aromatic and carboxyl groups, which are more reactive

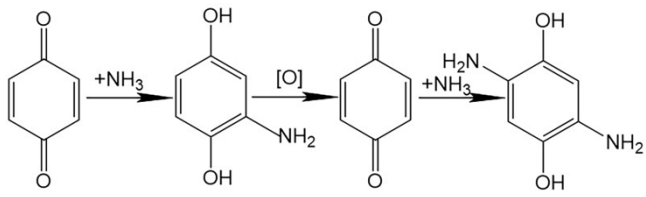

Figure 4 | Reaction model of NH_3 and quinine.

Table 2 | Concentrations of DBPs in influent and effluent

DBPs (μg/L)	Raw water	CUF water	O_3 water	BAC water
Tribromomethane (TBM)	0.67	1.25	2.55	0.96
Bromodichloromethane (BDCM)	17.35	17.95	14.14	5.50
Dibromochloromethane (DBCM)	8.84	10.15	10.97	5.62
Trichloromethane (TCM)	18.49	18.35	12.73	4.28
Monochloroacetic acid (MCAA)	–[a]	–	–	–
Dichloroacetic acid (DCAA)	14.82	16.73	17.52	6.43
Trichloroacetic acid (TCAA)	8.21	9.09	8.77	5.63
Monobromoacetic acid (MBAA)	1.70	1.96	2.09	–
Dibromoacetic acid (DBAA)	5.28	5.65	6.20	4.85

[a]The value was not detected.

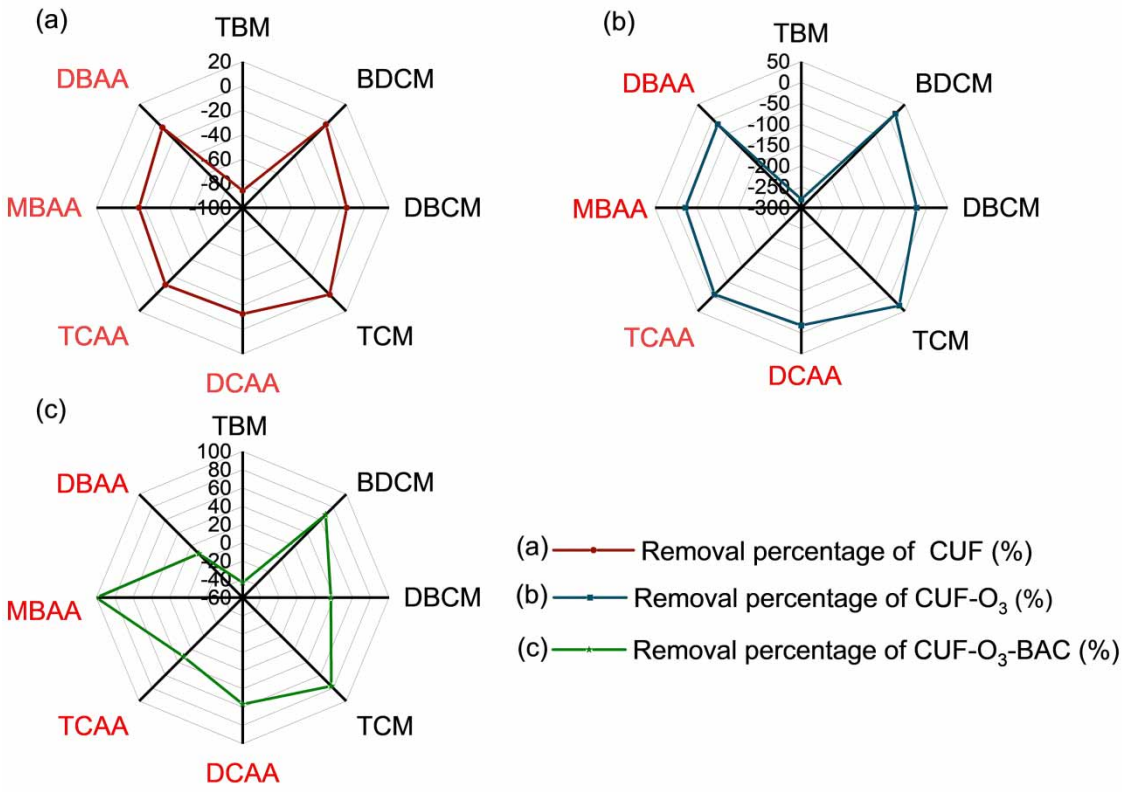

Figure 5 | Removal efficiencies of DBPs by the CUF–O_3–BAC integrated process.

to the formation of THMs and HAA_5 during chlorination (Xu *et al.* 2011). UF can effectively remove high MW fractions, which is propitious to the reaction of small and medium MW fractions with adequate chlorine, thus resulting in more DBPs. This also indicates that the CUF process has a tendency to increase the formation potentials of DBPs.

Figure 5(b) and Table 2 show that after CUF–O_3 treatment, the formation potentials of brominated DBPs increased significantly and those of chlorinated THMs decreased, while those of chlorinated HAA_5 did not change significantly. The removal efficiencies of BDCM and TCM reached 18.54 and 31.13%, respectively. The results indicated that ozone could reduce the formation risk of chlorinated THMs to a certain extent, but it was ineffective to reduce the formation risks of brominated THMs and HAA_5. This may be because ozonation transforms NOM from hydrophobic character to hydrophilic character and/or higher MW fractions to lower MW fractions, which are more likely to generate brominated DBPs during subsequent

chlorination (Hua & Reckhow 2013; Gao *et al.* 2020). Figure 5(c) shows that the removal efficiencies of TBM, BDCM, DBCM, TCM, DCAA, TCAA and DBAA are −43.51, 68.31, 36.43, 76.86, 56.61, 31.42 and 8.00%, respectively, whereas MBAA was not detected. Although the removal efficiency of TBM formation potential in BAC effluent was negative, the removal efficiency of TBM via the CUF–O_3–BAC process was still significantly improved compared to the CUF–O_3 unit. Therefore, the CUF–O_3–BAC process is an effective technology to remove THMs and HAA_5 precursors in drinking water treatment. Some studies have shown that GAC exhibits very high efficiency to adsorb small, neutral and hydrophobic molecules but relatively lower adsorption capacity for hydrophilic molecules (Fu *et al.* 2017). Therefore, hydrophilicity and low and medium MW fractions may be the major reason for the increase of brominated DBPs based on these theories.

3.6. TMP analysis

In the membrane treatment process, membrane flux and TMP are the most basic indicators of the membrane's operational stability and membrane fouling (Wang *et al.* 2020). Therefore, the long-term continuous operation of the membrane system was investigated by changing the membrane fluxes and recording the corresponding TMP values. During the experiment, the PLC system automatically recorded a TMP value every 5 min. To facilitate experimental analysis, the average value of data per 8 h was used to represent the variation of TMP. The variation of TMP under various membrane fluxes is shown in Figure 6(a). Figure 6(a) shows that the initial TMP values are 9.6, 12.3, 14.3 and 16 kPa at the fluxes of 60, 70, 80 and 90 L/(m^2·h), respectively. After 30 days of operation, the TMP increased to 15.2, 26.3, 30.3 and 37.5 kPa, respectively (Figure 6(a)). Now, the kinetic simulation of the relationship between TMP and time under various fluxes is carried out.

3.6.1. First-order kinetic simulation

The first-order kinetic equation is shown in the following equation:

$$\frac{\mathrm{TMP}}{\mathrm{TMP_0}} = \exp(-k_1 t) \tag{1}$$

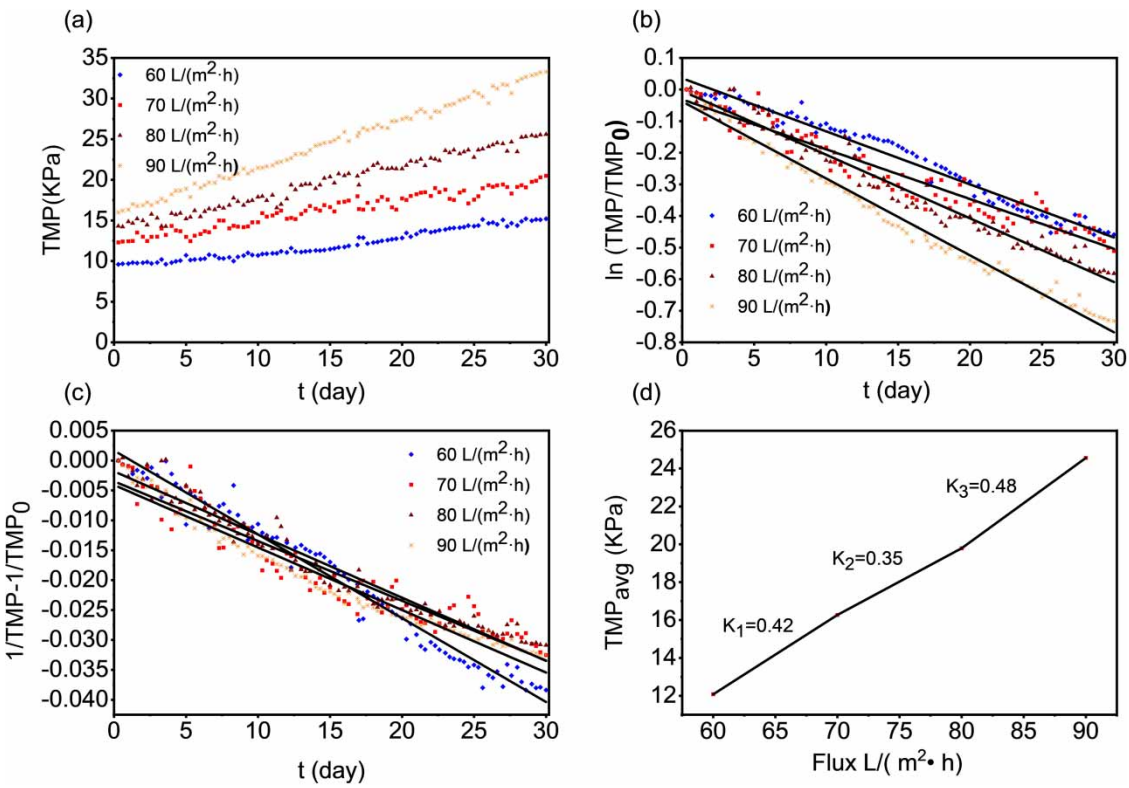

Figure 6 | (a) Variation of TMP with time under the flux of 60–90 L/(m^2·h), (b) the first-order kinetic growth model, (c) the second-order kinetic growth model and (d) the relationship between TMP_{avg} and flux.

where TMP (kPa) is the transmembrane pressure, TMP_0 (kPa) is the initial transmembrane pressure, t (day) is the time and k_1 represents the first-order kinetic constant of TMP with time.

Taking the logarithm of both sides of Equation (1) to get the following equation.

$$\ln\frac{TMP}{TMP_0} = -k_1 t \tag{2}$$

where $\ln(TMP/TMP_0)$ is the longitudinal coordinates, t is the horizontal ordinate and the linear regression is applied to investigate the relationship between $\ln(TMP/TMP_0)$ and t. The results are shown in Figure 6(b) and Table 3.

3.6.2. Second-order kinetic simulation

The second-order kinetic equation is shown in the following formula:

$$\frac{dTMP}{dt} = -k_2 TMP_0^2 \tag{3}$$

where k_2 is the second-order kinetic constant of TMP with time.

Integrating formula (3) to get the following formula:

$$\frac{1}{TMP} - \frac{1}{TMP_0} = k_2 t \tag{4}$$

where $(1/TMP) - (1/TMP_0)$ is the longitudinal coordinates, t is the horizontal ordinate and the linear regression is applied to investigate the relationship between $(1/TMP) - (1/TMP_0)$ and t. The results are shown in Figure 6(c) and Table 3.

According to the above linear fitting results, the correlation coefficients (R^2) of first-order dynamics and second-order dynamics were all greater than 0.9 under the four fluxes of 60, 70, 80 and 90 L/(m^2·h). The results indicated that the relationship of TMP with time accorded with both the first-order and second-order kinetics models. According to the fitting results in Figure 6(b) and Table 3, the rising rate of TMP did not increase with the increase of flux. On the contrary, when the flux was 70 L/(m^2·h), the growth rate of TMP was the slowest and the correlation coefficient was the smallest ($R^2 = 0.93$), which was also reflected in the second-order kinetics ($R^2 = 0.91$). It preliminarily indicated that the fouling extent of the membrane system was relatively the lowest under the flux of 70 L/(m^2·h).

The average TMP (TMP_{avg}) vs. flux plots are frequently used to determine critical and threshold fluxes from flux stepping experiments (Miller *et al.* 2014). To further determine the optimal flux, the relationship between TMP_{avg} and flux is plotted, and the results are shown in Figure 6(d). The curve of Figure 6(d) was divided into three sections and analyzed by linear regression, respectively. Figure 6(d) shows that the development of TMP_{avg} is particularly rapid with the increase of flux when the flux was >80 or <70 L/(m^2·h). On the contrary, the development of TMP_{avg} was relatively moderate under the condition of 70–80 L/(m^2·h). Therefore, we can draw a conclusion that the membrane system has relatively strong anti-fouling ability under the flux of 70 L/(m^2·h).

4. CONCLUSIONS

For the treatment of lake water with algae, this research adopted the CUF–O_3–BAC integrated process to treat East Taihu Lake water and first investigated the removal efficiencies of algae, COD_{Mn}, UV_{254}, NH_3-N and DBPs precursors. We

Table 3 | Kinetic linear fitting function

Flux, L/(m^2·h)	Linear fitting of first-order kinetics	R^2	Linear fitting of second-order kinetics	R^2
60	$y = -0.01679t + 0.03561$	0.97	$y = -0.0014t + 0.00167$	0.98
70	$y = -0.01575t - 0.03143$	0.93	$y = -9.98995 \times 10^{-4}t - 0.00347$	0.91
80	$y = -0.02014t - 0.00476$	0.97	$y = -0.00106t - 0.00181$	0.95
90	$y = -0.02434t - 0.03801$	0.99	$y = -0.00105t - 0.00409$	0.96

found that the integrated process had positive impaction of NH_3-N removal, which might be mainly determined by the formation of cake layer on the membrane surface, the nitrification of nitrifying bacteria and the influence of humic acid in raw water. However, further research is necessary to determine which factor dominates. The DBPs results indicated that the CUF unit tended to increase the formation potentials of THMs and HAA_5. This may be because the UF can effectively remove high MW fractions, which is more conducive to the reaction of small and medium MW fractions with sufficient chlorine, thus resulting in more DBPs. The formation potentials of brominated DBPs after CUF–O_3 effluent were significantly increased. This is attributed to ozone transforming NOM from hydrophobic character to hydrophilic character and/or higher MW fractions to lower MW fractions, which are considered brominated DBPs precursors. However, the CUF–O_3–BAC integrated process was an effective technology for the removal of THMs and HAA_5 precursors in drinking water treatment. Finally, we established the kinetic models of TMP and operation time and determined that the membrane system had relatively strong anti-fouling ability under the flux of 70 L/(m^2·h). However, we did not find out exactly what factors caused the relatively strong anti-fouling ability of the membrane system under the flux of 70 L/(m^2·h), which would continue to be observed and analyzed in the follow-up experiments.

ACKNOWLEDGEMENTS

This research has been supported by the 'Integration and comprehensive application of drinking water security technology in Suzhou' (No. 2017ZX07201001). The authors wish to gratefully acknowledge Lanzhou Jiaotong University and Tongji University for their support and assistance in this research.

DATA AVAILABILITY STATEMENT

All relevant data are included in the paper or its Supplementary Information.

REFERENCES

Bai, M., Zheng, Q., Zheng, W., Li, H., Lin, S., Huang, L. & Zhang, Z. 2019 •OH inactivation of cyanobacterial blooms and degradation of toxins in drinking water treatment system. *Water Res.* **54**, 144–152.

Chang, J., Chen, Z. L., Wang, Z., Shen, J. M., Chen, Q., Kang, J., Yang, L., Liu, X. W. & Nie, C. X. 2014 Ozonation degradation of microcystin-LR in aqueous solution: intermediates, byproducts and pathways. *Water Res.* **63**, 52–61.

Chaukura, N., Marais, S. S., Moyo, W., Mbali, N., Thakalekoala, L. C., Ingwani, T., Mamba, B. B., Jarvis, P. J. & Nkambule, T. T. 2020 Contemporary issues on the occurrence and removal of disinfection byproducts in drinking water – a review. *J. Environ. Chem. Eng.* **8** (2), 103659.

Chen, J. J., Yeh, H. H. & Tseng, I. C. 2009 Effect of ozone and permanganate on algae coagulation removal–pilot and bench scale tests. *Chemosphere* **74** (6), 840–846.

Chen, Z., Yang, B., Wen, Q. & Chen, C. 2020 Evaluation of enhanced coagulation combined with densadeg-ultrafiltration process in treating secondary effluent: organic micro-pollutants removal, genotoxicity reduction, and membrane fouling alleviation. *J. Hazard. Mater.* **396**, 122697.

Chen, B., Zhang, C., Wang, L., Yang, J. & Sun, Y. 2021 Removal of disinfection byproducts in drinking water by flexible reverse osmosis: efficiency comparison, fates, influencing factors, and mechanisms. *J. Hazard. Mater.* **401**, 123408.

de Oliveira, T. F., de Sousa Brandão, I. L., Mannaerts, M. C., Hauser-Davis, R. A., de Oliveira, A. A. F., Saraiva, A. C. F., de Oliveira, M. A. & Ishihara, J. H. 2020 Using hydrodynamic and water quality variables to assess eutrophication in a tropical hydroelectric reservoir. *J. Environ. Manage.* **256**, 109932.

Dong, F., Lin, Q., Li, C., Wang, L. & García, A. 2021 UV/chlorination process of algal-laden water: algal inactivation and disinfection byproducts attenuation. *Sep. Purif. Technol.* **257**, 117896.

Fan, C., Zhang, L., Qin, B., Hu, W., Gao, G. & Wang, J. 2004 Migration mechanism and quantification of biogenic elements in the sediment-water interface of Lake Taihu. *J. Lake Sci.* **16** (1), 10–20 (In Chinese).

Farré, M. J., Reungoat, J., Argaud, F. X., Rattier, M., Keller, J. & Gernjak, W. 2011 Fate of N-nitrosodimethylamine, trihalomethane and haloacetic acid precursors in tertiary treatment including biofiltration. *Water Res.* **45** (17), 5695–5704.

Feng, W. Y., Zhu, Y. R. & Wu, F. C. 2016 The fluorescent characteristics and sources of dissolved organic matter in water of Tai Lake, China. *Acta Sci. Circumst.* **36** (2), 475–482.

Fu, J., Lee, W. N., Coleman, C., Nowack, K., Carter, J. & Huang, C. H. 2017 Removal of disinfection byproduct (DBP) precursors in water by two-stage biofiltration treatment. *Water Res.* **123**, 224–235.

Gao, J., Proulx, F. & Rodriguez, M. J. 2020 Effects of ozonation on halogenated acetaldehydes and trihalomethanes formation: strategy of process control for a full-scale plant. *J. Water. Process. Eng.* **35**, 101205.

Han, X. G. & Huang, T. L. 2013 Removal efficiency of organics and total phosphorus in conventional process of water plants. *Chinese J. Environ. Eng.* **7** (5), 1616–1620 (In Chinese).

He, H. Y., Qiu, W., Liu, Y. L., Yu, H. R., Wang, L. & Ma, J. 2021 Effect of ferrate pre-oxidation on algae-laden water ultrafiltration: attenuating membrane fouling and decreasing formation potential of disinfection byproducts. *Water Res.* **190**, 116690.

Hua, G. & Reckhow, D. A. 2013 Effect of pre-ozonation on the formation and speciation of DBPs. *Water Res.* **47** (13), 4322–4330.

Kim, K. S., Oh, B. S., Kang, J. W., Chung, D. M., Cho, W. H. & Choi, Y. K. 2005 Effect of ozone and GAC process for the treatment of micropollutants and DBPs control in drinking water: pilot scale evaluation. *Ozone Sci. Eng.* **27**, 69–79.

Li, L., Zhang, W., Zhang, Y., Kuppers, S., Jin, L., Zhang, Y., Gao, N. & Zhang, D. 2019 Sulfate radical-based technology for the removal of 2-methylisoborneol and 2-methylisoborneol-producing algae in drinking water sources. *Chem. Eng. J.* **365**, 43–52.

Li, R., Gao, B., Wang, W., Yue, Q. & Wang, Y. 2020 Floc properties and membrane fouling in coagulation/ultrafiltration process for the treatment of Xiaoqing River: the role of polymeric aluminum-polymer dual-coagulants. *Chemosphere* **243**, 125391.

Lin, J. L., Hua, L. C., Hung, S. K. & Huang, C. 2018 Algal removal from cyanobacteria-rich waters by preoxidation-assisted coagulation–flotation: effect of algogenic organic matter release on algal removal and trihalomethane formation. *J. Environ. Sci.* **63**, 147–155.

Lin, Q., Dong, F., Li, C. & Cui, J. 2021 Disinfection byproduct formation from algal organic matters after ozonation or ozone combined with activated carbon treatment with subsequent chlorination. *J. Environ. Sci.* **104**, 233–241.

Liu, T., Lian, Y., Graham, N., Yu, W., Rooney, D. & Sun, K. 2017 Application of polyacrylamide flocculation with and without alum coagulation for mitigating ultrafiltration membrane fouling: role of floc structure and bacterial activity. *Chem. Eng. J.* **307**, 41–48.

Lui, Y. S., Qiu, J. W., Zhang, Y. L., Wong, M. H. & Liang, Y. 2011 Algal-derived organic matter as precursors of disinfection by-products and mutagens upon chlorination. *Water Res.* **45**, 1454–1462.

Lundqvist, J., Andersson, A., Johannisson, A., Lavonen, E., Mandava, G., Kylin, H. & Oskarsson, A. 2019 Innovative drinking water treatment techniques reduce the disinfection-induced oxidative stress and genotoxic activity. *Water Res.* **155**, 182–192.

Lzydorczyk, K., Carpentier, C., Mrówczyński, J., Wagenvoort, A., Jurczak, T. & Tarczyńska, M. 2009 Establishment of an alert level framework for cyanobacteria in drinking water resources by using the algae online analyser for monitoring cyanobacterial chlorophyll *a*. *Water Res.* **43** (4), 989–996.

Ma, J. & Liu, W. 2002 Effectiveness and mechanism of potassium ferrate (VI) preoxidation for algae removal by coagulation. *Water Res.* **36** (4), 871–878.

Mazhar, M. A., Khan, N. A., Ahmed, S., Khan, A. H., Hussain, A., Changani, F., Yousefi, M. & Vambol, V. 2020 Chlorination disinfection by-products in municipal drinking water – a review. *J. Cleaner Prod.* **273**, 123159.

Meng, Q. J., Zhang, Y., Feng, Q. Y. & Zhang, S. S. 2011 Effect of humic acids on migration and transformation of NH_4^+-N in saturated aquifer. *Environ. Sci.* **32** (11), 3357–3364 (In Chinese).

Miller, D. J., Kasemset, S., Paul, D. R. & Freeman, B. D. 2014 Comparison of membrane fouling at constant flux and constant transmembrane pressure conditions. *J. Membr. Sci.* **454**, 505–515.

Ministry of environmental protection 2015 *Water Quality-Determination of Haloacetic Acids-Gas Chromatography.* HJ 758-2015 (In Chinese).

Pan, S., An, W., Li, H., Su, M., Zhang, J. & Yang, M. 2014 Cancer risk assessment on trihalomethanes and haloacetic acids in drinking water of China using disability-adjusted life years. *J. Hazard. Mater.* **280**, 288–294.

Prasert, T., Ishii, Y., Kurisu, F., Musikavong, C. & Phungsai, P. 2021 Characterization of lower Phong river dissolved organic matters and formations of unknown chlorine dioxide and chlorine disinfection by-products by Orbitrap mass spectrometry. *Chemosphere* **265**, 128653.

Qi, J., Lan, H., Liu, R., Miao, S., Liu, H. & Qu, J. 2016 Prechlorination of algae-laden water: the effects of transportation time on cell integrity, algal organic matter release, and chlorinated disinfection byproduct formation. *Water Res.* **102**, 221–228.

Rangesh, S. & Sorial, G. A. 2011 Treatment of taste and odor causing compounds 2-methyl isoborneol and geosmin in drinking water: a critical review. *J. Environ. Sci.* **23**, 1–13.

Stevenson, F. J. Translated by Xia, R. 1994 *Humus Chemistry*. Beijing Agricultural University Press, Beijing, pp. 75–76 (In Chinese).

Sun, Y., Angelotti, B., Brooks, M., Dowbiggin, B., Evans, P. J., Devins, B. & Wang, Z. W. 2018 A pilot-scale investigation of disinfection by-product precursors and trace organic removal mechanisms in ozone-biologically activated carbon treatment for potable reuse. *Chemosphere* **210**, 539–549.

Tabatabai, S. A. A., Schippers, J. C. & Kennedy, M. D. 2014 Effect of coagulation on fouling potential and removal of algal organic matter in ultrafiltration pretreatment to seawater reverse osmosis. *Water Res.* **59** (283), 283–294.

Thomson-Laing, G., Puddick, J. & Wood, S. A. 2020 Predicting cyanobacterial biovolumes from phycocyanin fluorescence using a handheld fluorometer in the field. *Harmful Algae* **97**, 101869.

Thostenson, J. O., Mourouvin, R., Hawkins, B. T., Ngaboyamahina, E., Sellgren, K. L., Parker, C. B., Deshusses, M. A., Stoner, B. R., Glass, J. T., Watson, K., Farré, M. J. & Knight, N. 2018 Improved blackwater disinfection using potentiodynamic methods with oxidized boron-doped diamond electrodes. *Water Res.* **140**, 191–199.

Wang, W. L., Cai, Y. Z., Hu, H. Y., Chen, J., Wang, J., Xue, G. & Wu, Q. Y. 2019 Advanced treatment of bio-treated dyeing and finishing wastewater using ozone-biological activated carbon: a study on the synergistic effects. *Chem. Eng. J.* **359**, 168–175.

Wang, Y., Ju, L., Xu, F., Tian, L., Jia, R., Song, W., Li, Y. & Liu, B. 2020 Effect of a nanofiltration combined process on the treatment of high-hardness and micropolluted water. *Environ. Res.* **182**, 109063.

Wang, X. X., Liu, B. M., Lu, M. F., Li, Y. P., Jiang, Y. Y., Zhao, M. X., Huang, Z., Pan, Y., Miao, H. & Ruan, W. Q. 2021 Characterization of algal organic matter as precursors for carbonaceous and nitrogenous disinfection byproducts formation: comparison with natural organic matter. *J. Environ. Manage.* **282**, 111951.

Watson, K., Farré, M. J., Leusch, F. D. & Knight, N. 2018 Using fluorescence-parallel factor analysis for assessing disinfection by-product formation and natural organic matter removal efficiency in secondary treated synthetic drinking waters. *Sci. Total Environ.* **640**, 31–40.

Wongcharee, S., Aravinthan, V. & Erdei, L. 2020 Removal of natural organic matter and ammonia from dam water by enhanced coagulation combined with adsorption on powdered composite nano-adsorbent. *Environ. Technol. Innov.* **17**, 100557.

Xu, B., Ye, T., Li, D. P., Hu, C. Y., Lin, Y. L., Xia, S. J., Tian, F. X. & Gao, N. Y. 2011 Measurement of dissolved organic nitrogen in a drinking water treatment plant: size fraction, fate, and relation to water quality parameters. *Sci. Total Environ.* **409** (6), 1116–1122.

Xu, D., Bai, L., Tang, X., Niu, D., Luo, X., Zhu, X., Li, G. & Liang, H. 2019 A comparison study of sand filtration and ultrafiltration in drinking water treatment: removal of organic foulants and disinfection by-product formation. *Sci. Total Environ.* **691**, 322–331.

Yan, M., Wang, D., Ma, X., Ni, J. & Zhang, H. 2010 THMs precursor removal by an integrated process of ozonation and biological granular activated carbon for typical Northern China water. *Sep. Purif. Technol.* **72**, 263–268.

Yang, L., She, Q., Wan, M. P., Wang, R., Chang, V. W. C. & Tang, C. Y. 2017 Removal of haloacetic acids from swimming pool water by reverse osmosis and nanofiltration. *Water Res.* **116**, 116–125.

Yin, Q., Guo, X., Gui, B., Chen, Y. & Dong, B. 2019 Pilot experiment of ultrafiltration-ozone-biological activated carbon advanced process for treatment of Taihu lake. *Water Wastewater Eng.* **45** (11), 9–12 (In Chinese).

Yu, H., Li, X., Chang, H., Zhou, Z., Zhang, T., Yang, Y., Li, G., Ji, H., Cai, C. & Liang, H. 2020 Performance of hollow fiber ultrafiltration membrane in a full-scale drinking water treatment plant in China: a systematic evaluation during 7-year operation. *J. Membr. Sci.* **613**, 118469.

Zhang, Z. 2000 *Drainage Engineering*. China Architecture & Building Press, Beijing, pp. 306–307 (In Chinese).

Zhang, X. R. B. J. & Bai, R. 2003 Mechanisms and kinetics of humic acid adsorption onto chitosan-coated granules. *J. Colloid Interface Sci.* **264** (1), 30–38.

Zhang, X., Chen, Z., Shen, J., Zhao, S., Kang, J., Chu, W., Zhou, Y. & Wang, B. 2020 Formation and interdependence of disinfection byproducts during chlorination of natural organic matter in a conventional drinking water treatment plant. *Chemosphere* **242**, 125227.

Zhao, Z., Sun, W., Ray, A. K., Mao, T. & Ray, M. B. 2020 Coagulation and disinfection by-products formation potential of extracellular and intracellular matter of algae and cyanobacteria. *Chemosphere* **245**, 125669.

Zhu, M., Gao, N., Chu, W., Zhou, S., Zhang, Z., Xu, Y. & Dai, Q. 2015 Impact of pre-ozonation on disinfection by-product formation and speciation from chlor(am)ination of algal organic matter of *Microcystis aeruginosa*. *Ecotoxicol. Environ. Saf.* **120**, 256–262.

First received 18 January 2021; accepted in revised form 13 September 2021. Available online 7 October 2021